

UC Berkeley

Technical Completion Reports

Title

Application of acoustic pressure waves in aquifer remediation and mobilization of entrapped organic liquids

Permalink

<https://escholarship.org/uc/item/8ws4t9z1>

Authors

Chrysikopoulos, Constantinos V
Vogler, Eric T

Publication Date

2002-10-01

Application of Acoustic Pressure Waves in Aquifer

Remediation and Mobilization of Entrapped

Organic Liquids

BY

CONSTANTINOS V. CHRYSIKOPOULOS AND ERIC T. VOGLER

*Department of Civil and Environmental Engineering
University of California, Irvine, CA 92697-2175*

TECHNICAL COMPLETION REPORT

Project Number UCAL-WRC-W-938

October, 2002

University of California Water Resources Center

ABSTRACT

The effect of acoustic waves on the transport of a conservative tracer and the dissolution of dense nonaqueous phase liquids (DNAPLs) in a water saturated column packed with glass beads was investigated. It was observed from the experimental data that the addition of acoustic waves, in the frequency range between 60 to 245 Hz, to a steady background pressure gradient, enhances solute transport compared to the base case consisting of only a background pressure gradient. Furthermore, it was found that the effective velocity of the solute is approximately inversely proportional to the frequency of the acoustic wave. In addition, acoustic waves with pressure amplitudes ranging from 0 to 1625 Pa and frequencies ranging from 0 to 285 Hz were observed to increase the effluent dissolved trichloroethene (TCE) concentration, where TCE was used as the DNAPL, compared to the case where dissolution without acoustic waves was monitored. The increased effluent dissolved TCE concentration is attributed to an increase in mass flux from the dissolving TCE blobs due to increased effective pore water velocity caused by acoustic waves.

KEY WORDS: Acoustic waves, remediation, organic liquids, dissolution, transport.

TABLE OF CONTENTS

	<u>Page</u>
COVER PAGE	i
ABSTRACT	ii
TABLE OF CONTENTS	iii
LIST OF FIGURES	iv
INTRODUCTION	1
SOLUTE TRANSPORT IN POROUS MEDIA	3
METHODS	5
Bromide Tracer Experiment	5
DNAPL Dissolution Experiment	6
RESULTS	9
Acoustic Enhanced Transport	9
Acoustic Enhanced DNAPL Dissolution	12
SUMMARY	16
REFERENCES	17

LIST OF FIGURES

	<u>Page</u>
Figure 1: Experimental apparatus (Vogler and Chrysikopoulos, 2002).	6
Figure 2: Background base case dissolution experiment showing amount of time necessary to reach a quasi steady effluent concentration and relative experimental error.	8
Figure 3: Tracer (Br^-) concentration breakthrough data (solid circles) and fitted model (solid curve) in the absence of acoustic pressure (base case) compared to breakthrough data (open circles) and fitted model (dashed curve) obtained in the presence of acoustic pressure at 60 Hz (Vogler and Chrysikopoulos, 2002).	10
Figure 4: Experimentally determined effective velocity (solid squares) for various acoustic pressure frequencies. The dashed line represents the case of no acoustic waves present (base case) (Vogler and Chrysikopoulos, 2002).	10
Figure 5: Effective dispersion coefficient (open squares) for various acoustic pressure frequencies. The dashed line represents the case of no acoustic waves present (base case) (Vogler and Chrysikopoulos, 2002).	11
Figure 6: Example experiment showing the effect of acoustic frequency on effluent concentration for an acoustic source pressure amplitude of 812 Pa at 225 Hz. Closed circles represent the base case (no acoustic pressure) and open circles in the grey region represent acoustic portions of the experiment.	13
Figure 7: Effect of acoustic frequency on percent change in effluent concentration for a constant acoustic source pressure amplitude of 812 Pa. Circles with dotted lines represent experiments conducted with 1 mm beads and squares with solid lines represent experiments conducted with 2 mm bead column packings.	13
Figure 8: Effluent acoustic pressures for a constant acoustic source pressure amplitude of 812 Pa for the range of frequencies used in dissolution experiments. Circles with dotted lines represent experiments conducted with 1 mm beads and squares with solid lines represent experiments conducted with 2 mm bead column packings.	14
Figure 9: Effect of acoustic source pressure amplitude on percent change in effluent concentration for a constant acoustic frequency of 245 Hz. Circles with best fit dotted lines represent experiments conducted with 1 mm beads and squares with solid best fit lines represent experiments conducted with 2 mm bead column packings.	15

Various aspects of contaminant transport enhancement in porous media have been extensively explored in recent years by environmental engineers and scientists who design remediation methods for contaminated subsurface formations. For example, remediation techniques for groundwater and soil contaminated by nonaqueous phase liquids (NAPLs), often employ surfactants to reduce surface tension and enhance mobilization of NAPLs (Mason and Kueper, 1996; Fortin et al., 1997), or employ cosolvents and humic substances to increase the solubility of slightly soluble NAPLs (Brandes and Farley, 1993; Li et al., 1996; Tatalovich et al., 2000). Furthermore, bioremediation techniques employ bacteria that enhance contaminant degradation (Chaudhry, 1994). Unfortunately, all of these remediation methods introduce additional contaminants into the subsurface. In contrast, the use of acoustic waves in groundwater remediation does not lead to further contamination of the subsurface environment. Acoustic waves have been successfully employed in enhanced oil recovery operations (Beresnev and Johnson, 1994) and perhaps can also be used to reduce the time and cost of groundwater remediation.

The novel idea of using acoustic waves as a potential remediation method has only recently received attention. Since Biot's fundamental work (Biot, 1956a,b) on elastic waves in saturated porous media, there have been significant developments on sound propagation in saturated porous media as well as porous media saturated by two immiscible fluids (Santos et al., 1990; Parra and Xu, 1994; Geerits and Kelder, 1997). However, to our knowledge, the possible enhancement of solute transport in water saturated porous media due to the presence of acoustic waves has not yet been investigated.

In addition to the possible enhancement of solute transport by acoustic waves, the dissolution of dense NAPLs (DNAPLS) may also be enhanced. If the addition of acoustic waves can enhance solute transport they will also affect the interstitial pore water velocity. Consequently, it is reasonable to expect that acoustic waves can lead to dissolution enhancement of residual NAPL in porous media due to the dependence of dissolution on the interstitial pore water velocity (Imhoff et al., 1994; Powers et al., 1992; Zhou et al., 2000; Chrysikopoulos, 1995; Chrysikopoulos et al., 2000; Vogler and Chrysikopoulos, 2001; Dela Barre et al., 2002, to mention a few). A novel “clean” remediation method is proposed in this study that uses acoustic waves to enhance DNAPL dissolution rates by increasing the NAPL-water interphase mass transfer. This work focuses on the experimental quantification of acoustic enhancement to both, solute transport and DNAPL dissolution in porous media.

SOLUTE TRANSPORT IN POROUS MEDIA

The one-dimensional transport of a non-sorbing solute or a conservative tracer in water saturated porous media under a constant hydraulic gradient can be described by the following linear, second-order partial differential equation:

$$\frac{\partial C(x, t)}{\partial t} = -U_e \frac{\partial C(x, t)}{\partial x} + D_e \frac{\partial^2 C(x, t)}{\partial x^2}, \quad (1)$$

where C is the liquid phase solute concentration [M/L³]; t is time [t]; U_e is the effective interstitial fluid velocity [L/t]; and D_e is the effective hydrodynamic dispersion coefficient [L²/t]. The effective interstitial fluid velocity is defined as

$$U_e = U + U^*, \quad (2)$$

where U is the steady state, background interstitial fluid velocity [L/t] and U^* is the additional velocity component attributed to acoustic pressure [L/t]. Similarly, the effective dispersion coefficient is defined

$$D_e = D + D^* = (U + U^*)\alpha_L + \mathcal{D}_e = U_e\alpha_L + \mathcal{D}_e, \quad (3)$$

where $D = U\alpha_L + \mathcal{D}_e$ is the hydrodynamic dispersion coefficient [L²/t]; α_L is the longitudinal dispersivity [L]; $\mathcal{D}_e = \mathcal{D}/\tau^*$ is the effective molecular diffusion coefficient [L²/t] (where \mathcal{D} is the molecular diffusion coefficient [L²/t], and $\tau^* > 1$ is the tortuosity coefficient [-]); and D^* is the additional dispersion component attributed to acoustic pressure [L²/t]. It should be noted that the concept of effective parameters has been applied in numerous groundwater flow and solute transport studies (Valocchi, 1989; Chrysikopoulos et al., 1990, 1992; Kabala and Sposito, 1991; Chrysikopoulos, 1995)

For a finite system, the following initial and boundary conditions can be used (Kreft and Zuber, 1978)

$$C(x, 0) = 0, \quad (4)$$

$$-D_e \frac{\partial C(0, t)}{\partial x} + U_e C(0, t) = M_0 \delta(t), \quad (5)$$

$$-D_e \frac{\partial C(L, t)}{\partial x} + U_e C(L, t) = U_e C_f, \quad (6)$$

where $M_0 = M/A\theta$ is the mass injected over the cross sectional area of the column (where M is the injected mass [M], A is the cross sectional area of the porous medium [L^2], and θ is porosity [-]); δ is the Dirac delta function [1/t]; and C_f is the effluent flux concentration [M/ L^3]. It should be noted that C corresponds to the *in situ* or resident concentration, whereas C_f is the flux concentration defined as the ratio of the solute mass flux to the volumetric fluid flux (Kreft and Zuber, 1978). Initial condition (4) establishes a zero background concentration. Boundary condition (5) describes the flux influent pulse concentration. Boundary condition (6) describes the flux effluent solute concentration at the end of the packed column $x = L$. The solution to the governing equation (1) subject to conditions (4)–(6), for the effluent concentration of a one-dimensional packed column of length L is obtained by straightforward Laplace transform procedures to yield (Vogler and Chrysikopoulos, 2002):

$$C(x, t) = \frac{xM_0}{2U_e t} \left(\frac{1}{\pi D_e t} \right)^{1/2} \exp \left[-\frac{1}{4D_e t} \left(x - U_e t \right)^2 \right]. \quad (7)$$

Bromide Tracer Experiment

The effect of acoustic waves on solute transport in water saturated porous media was investigated in this study by injecting a bromide tracer pulse into a 30 cm long glass laboratory column with a 2.5 cm inner diameter (Kimble Kontes, New Jersey). The column was packed with 2 mm diameter glass beads (Fisher Scientific, Pennsylvania) that were retained in the column with teflon screens placed on both the influent and effluent sides of the column. The teflon column end caps were milled to accommodate 1/4 inch stainless steel fittings (Swageloc) for 3/8 inch semi-rigid plastic tubing (Fisher Scientific, Pennsylvania). Constant flow of degassed Millipore water at a rate of 1.48 ml/min was maintained through the packed column with a microprocessor pump drive (Cole Palmer Instrument Co., Illinois). Acoustic pressure was introduced into the column through the plastic tubing with a specially designed reservoir containing a pressure transducer (TST37; Clark Sythesis, Colorado). The frequency of the acoustic pressure oscillation was controlled by a frequency generator (LG Precision, California). Acoustic pressure levels were controlled by an amplifier (Lab Gruppen, Sweden) and measured with a PCB106b pressure sensor in conjunction with a signal conditioner (PCB Piezotronics, Inc., New York) and a digital multimeter (Metex, Korea). Effluent samples were collected from a dedicated needle (sampling port) within the effluent tube. A complete schematic of the experimental apparatus employed in this study is shown in Figure 1.

The tracer solution was prepared by dissolving 256 mg of potassium bromide salt (KBr) (Fisher Scientific, Pennsylvania) into a liter of total solution volume to yield a final Br^- concentration of 172 mg/L. Alkali halides are the most commonly used salts for subsurface fluid tracing (Chrysikopoulos, 1993). A slug of 0.6 mL of the tracer solution was instantaneously injected into the column by a side injection port midway down the column. Sample effluent volumes of 0.8 mL were collected at regular intervals using disposable 1.0 mL tuberculin plastic syringes (Becton Dickinson & Co., New Jersey). The Br^- concentrations of the liquid samples were determined using a Dionex DX-120 ion chromatograph (Dionex, California). The base case experiment was first conducted to determine background U , and α_L in the absence of acoustic waves (0 Hz). Subsequently, flowthrough experiments were conducted using the same procedure described for the base case, but in the presence of acoustic waves at ten different preselected acoustic frequencies.

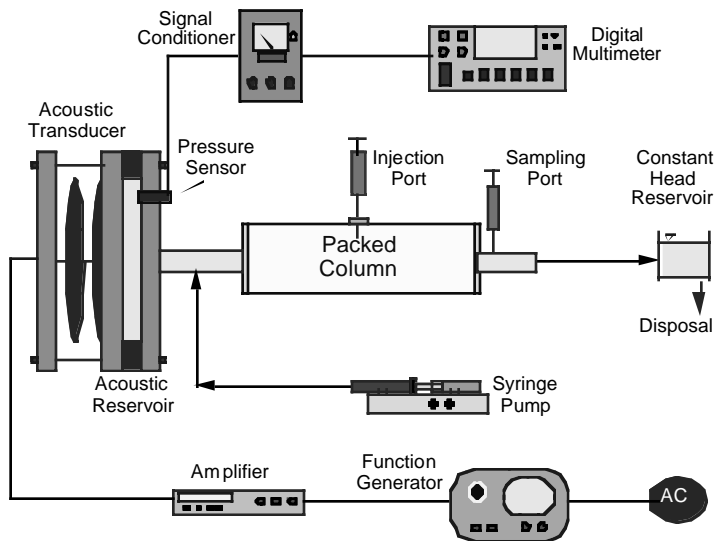


Figure 1: Experimental apparatus (Vogler and Chrysikopoulos, 2002).

DNAPL Dissolution Experiment

The effect of acoustic pressure waves on mass transfer from a DNAPL blob in saturated porous media was investigated by conducting flowthrough dissolution experiments in a 30 cm long glass laboratory column with a 2.5 cm inner diameter (Kimble Kontes, New Jersey). The column was packed with either 1 or 2 mm diameter soda lime glass beads with a density of 2.33 g/cc (Fisher Scientific, Pennsylvania). The beads were retained in the column using teflon screens and end caps on both the influent and effluent sides of the column. The teflon column end caps were milled to accommodate 1/4 inch stainless steel fittings (Swageloc) for 3/8 inch semi-rigid plastic tubing (Fisher Scientific, Pennsylvania). Constant flow of degassed Millipore water at 3.25 ml/min was maintained through the packed column with a microprocessor pump drive (Cole

Palmer Instrument Co., Illinois). Acoustic pressure was introduced into the column using a custom designed acoustic reservoir containing a pressure transducer (TST37; Clark Sythesis, Colorado). The frequency of acoustic pressure oscillation was controlled by a frequency generator (LG Precision, California). Acoustic pressure levels were controlled by an amplifier (Lab Gruppen, Sweden) and measured using PCB106b pressure sensors (PCB Piezotronics, Inc., New York). One pressure sensor was installed in the acoustic reservoir to measure the acoustic source pressure and the other sensor was installed in the effluent line, just after the packed column, to measure the effluent pressure. Influent pressure was also measured just before the packed column by interchanging the pressure sensor between the effluent and influent locations. Pressure sensor measurements were made using a signal conditioner (PCB Piezotronics, Inc., New York) in addition to a digital multimeter (Metex, Korea) and oscilloscope (EZ Digital Co., Ltd, Korea).

Effluent samples (0.15 ml) were collected from a dedicated needle within the effluent tube (sample port) at regular 10 minute intervals using disposable 1.0 ml tuberculin plastic syringes (Becton Dickinson & Co., New Jersey). The samples were immediately introduced into 2 ml autosampler vials (Kimble Glass, New Jersey) previously containing a known mass and volume of n-Pentane (Fisher Scientific, Pennsylvania) which was also used as an extraction solvent for gas chromatography analysis. The TCE concentrations of the liquid samples were determined using a Hewlett Packard 5890 Series II gas chromatograph with an electron capture detector.

DNAPL dissolution experiments were initiated by injecting 0.05 ml of TCE (Fisher Scientific, Pennsylvania) dyed red with oil red EGN (Aldrich Chemical Co., Wisconsin) into a side injection port in the middle of the packed column and allowed to equilibrate to flow conditions within the packed column. Several background base case experiments (without acoustic pressure) suggested that 5 pore volumes are sufficient to achieve a relatively steady effluent concentration. Observed base case effluent concentrations for

the column with 2 mm beads are shown in Figure 2. Clearly, within 5 pore volumes the effluent concentration increases from a zero initial concentration to a relatively constant concentration (~ 0.01 g/L). The observed scatter in the effluent concentration was considered representative of the overall experimental error. To assess the effect of acoustic waves on NAPL dissolution, a range of acoustic frequencies and amplitudes were applied at a 60 minute intervals following a 60 minute interval of flow without acoustic pressure.

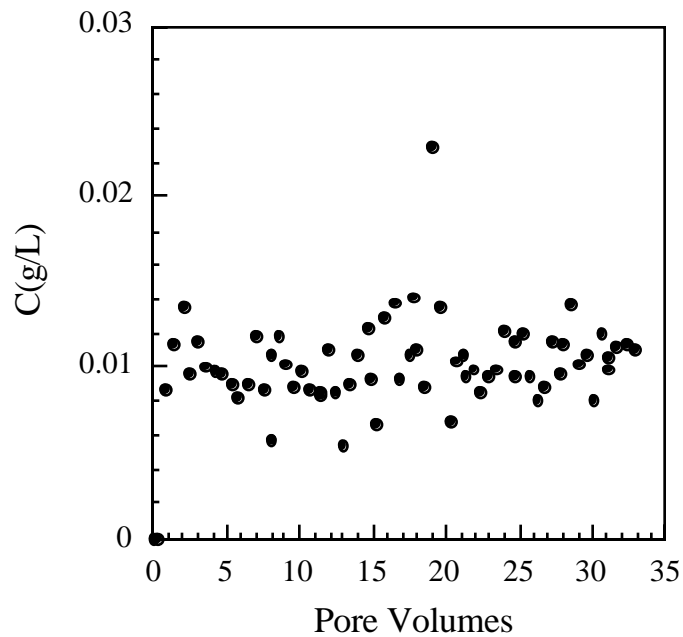


Figure 2: Background base case dissolution experiment showing amount of time necessary to reach a quasi steady effluent concentration and relative experimental error.

Acoustic Enhanced Transport

The experimental Br^- breakthrough data for the base case are presented in Figure 3 (solid circles) together with the breakthrough data collected in the presence of acoustic waves with frequency 60 Hz (open circles). Clearly, the presence of acoustic waves leads to a faster breakthrough of the conservative tracer. The nonlinear regression subroutine *mrqmin* (Press et al., 1992) was employed to estimate the dispersivity of the packed column $\alpha_L = 0.117$ cm and the steady state background interstitial fluid velocity $U = 0.644$ cm/min, by fitting the analytical solution derived in this work, (7), to the experimental breakthrough data for the base case. The effective molecular diffusion coefficient of Br^- used for the nonlinear regression procedure is $\mathcal{D}_e = \mathcal{D}/\tau^* = 8.62 \times 10^{-4}$ cm²/min, or equivalently $\mathcal{D} = 1.2067 \times 10^{-3}$ cm²/min (Domenico and Schwartz, 1990), and $\tau^* = 1.4$ (de Marsily, 1986). Subsequently, the same fitting procedure was employed to determine the effective velocity (U_e), using a fixed value of α_L , for each of the ten different breakthrough data sets collected in this study in the presence of acoustic waves. The estimated effective velocity for the base case and the ten different frequencies ranging from 0 to 245 Hz at a constant pressure amplitude of 565 Pa are shown in Figure 4. The estimated effective dispersion coefficient for the base case and the ten different acoustic frequencies are shown in Figure 5. It should be noted that the values in Figure 5 were obtained directly from (3) using the U_e values presented in Figure 4.

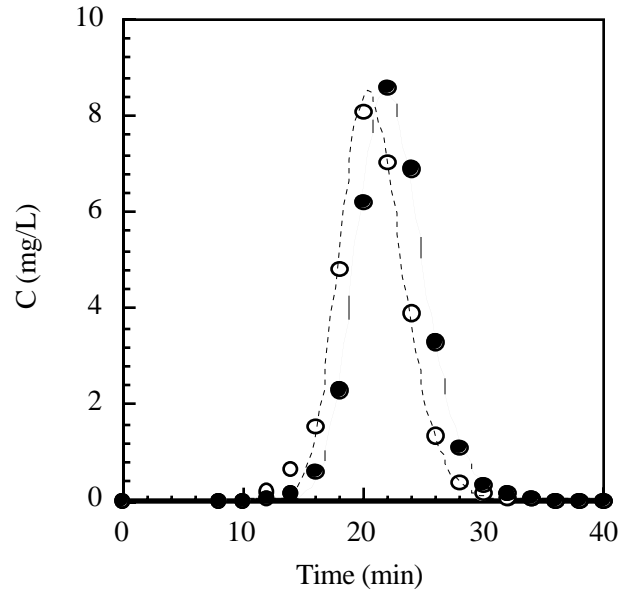


Figure 3: Tracer (Br^-) concentration breakthrough data (solid circles) and fitted model (solid curve) in the absence of acoustic pressure (base case) compared to breakthrough data (open circles) and fitted model (dashed curve) obtained in the presence of acoustic pressure at 60 Hz (Vogler and Chrysikopoulos, 2002).

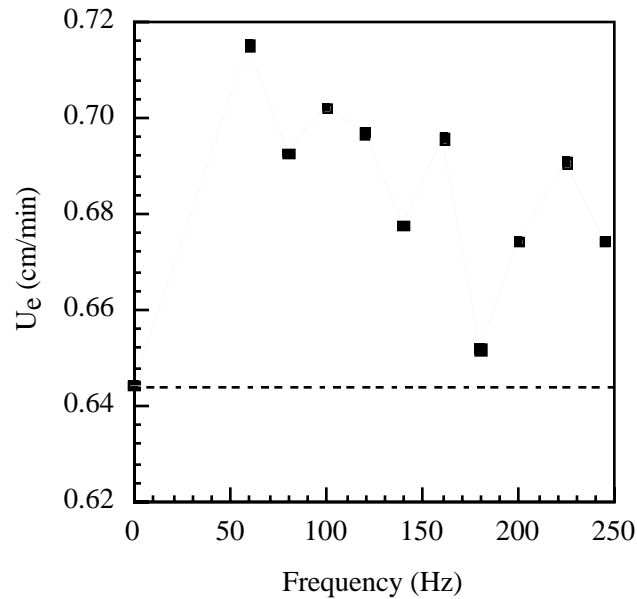


Figure 4: Experimentally determined effective velocity (solid squares) for various acoustic pressure frequencies. The dashed line represents the case of no acoustic waves present (base case) (Vogler and Chrysikopoulos, 2002).

Obviously, acoustic waves, particularly at low frequencies, enhance the tracer velocity and consequently enhance tracer dispersion (see Equation (3)). It should also be noted that due to experimental limitations in the low acoustic frequency range, no characteristic acoustic wave frequency was found to produce a maximum enhancement of the tracer transport. However, the enhanced interstitial fluid velocity appears to be approximately inversely proportional to the acoustic frequency.

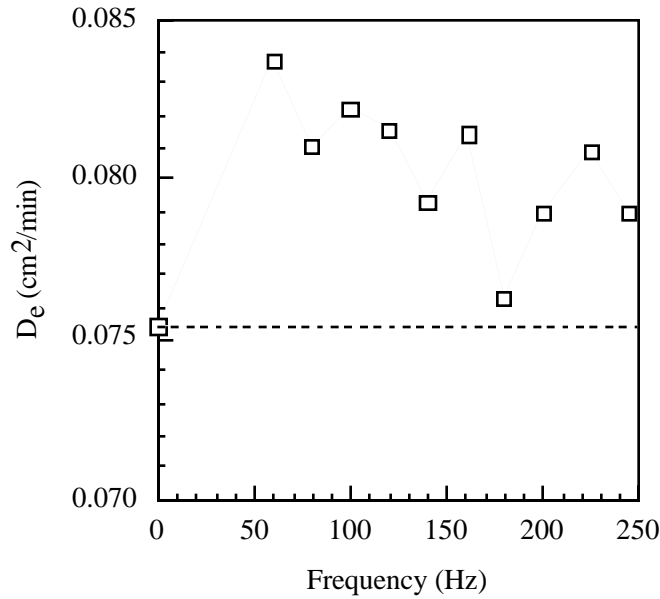


Figure 5: Effective dispersion coefficient (open squares) for various acoustic pressure frequencies. The dashed line represents the case of no acoustic waves present (base case) (Vogler and Chrysikopoulos, 2002).

Acoustic Enhanced DNAPL Dissolution

Dissolution experiments were conducted for frequencies ranging from 0 (base case) to 285 Hz at a constant source acoustic pressure amplitude of 812 Pa for both 1 and 2 mm beads. Experiments were also conducted at a constant frequency of 245 Hz for acoustic source pressures ranging from 0 (base case) to 1,625 Pa. An example of one experiment, with 2 mm beads, for a constant acoustic pressure amplitude of 812 Pa at 225 Hz, is shown in Figure 6. It should be noted that the effluent concentrations, after the acoustic pressure is discontinued, returns to base case values.

Results for the effect of frequency and acoustic pressure on dissolution are expressed as the average change in effluent concentration (ΔC) as a percent increase compared to the corresponding base case. The overall percent change in concentration was determined by averaging the last 3 samples from the acoustic case \overline{C}_{ac} and the last 3 samples from the corresponding base case \overline{C}_{bc} , then calculating the percent difference as

$$\Delta C = \frac{\overline{C}_{ac} - \overline{C}_{bc}}{\overline{C}_{bc}} \times 100. \quad (8)$$

The effect of acoustic waves at a constant acoustic cell source pressure amplitude of 812 Pa for frequencies ranging from 0 to 285 Hz for 1 and 2 mm beads were found to enhance dissolution, represented by increases in effluent concentration, of the TCE source (Figure 7). The greatest change in concentration, for both 1 and 2 mm bead column packings, occurred at 225 Hz at 120 and 96 %, respectively. Two distinct peaks in ΔC were found at 161 and 225 Hz for both bead sizes. The highest frequency used, 285 Hz, also resulted in an increase in ΔC at 61 and 45 % for the 1 and 2 mm beads, respectively (Figure 7). There was an additional peak in ΔC of 25 % for the 2 mm beads at 75 Hz that was not observed for the 1 mm beads (Figure 7). Except for frequencies below 161 Hz and 275 Hz, ΔC was observed to be greater for 1 mm beads than the 2 mm beads.

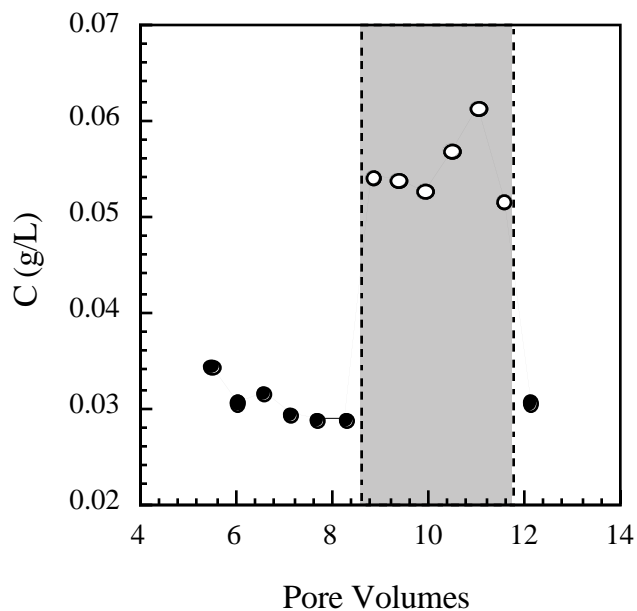


Figure 6: Example experiment showing the effect of acoustic frequency on effluent concentration for an acoustic source pressure amplitude of 812 Pa at 225 Hz. Closed circles represent the base case (no acoustic pressure) and open circles in the grey region represent acoustic portions of the experiment.

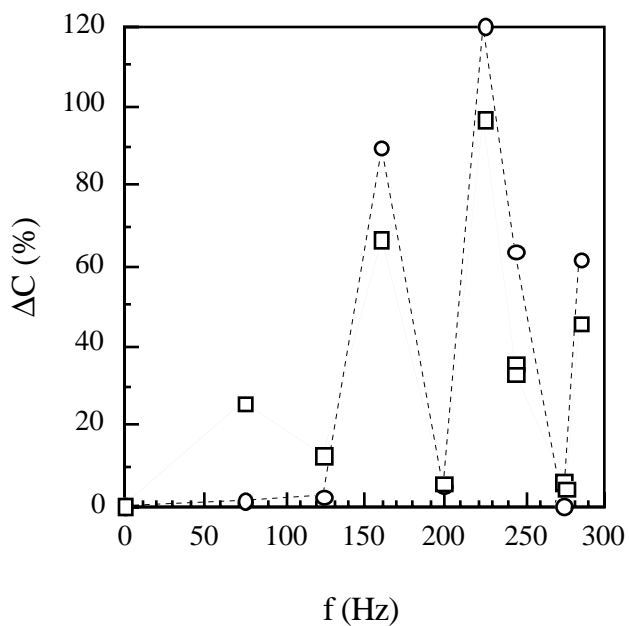


Figure 7: Effect of acoustic frequency on percent change in effluent concentration for a constant acoustic source pressure amplitude of 812 Pa. Circles with dotted lines represent experiments conducted with 1 mm beads and squares with solid lines represent experiments conducted with 2 mm bead column packings.

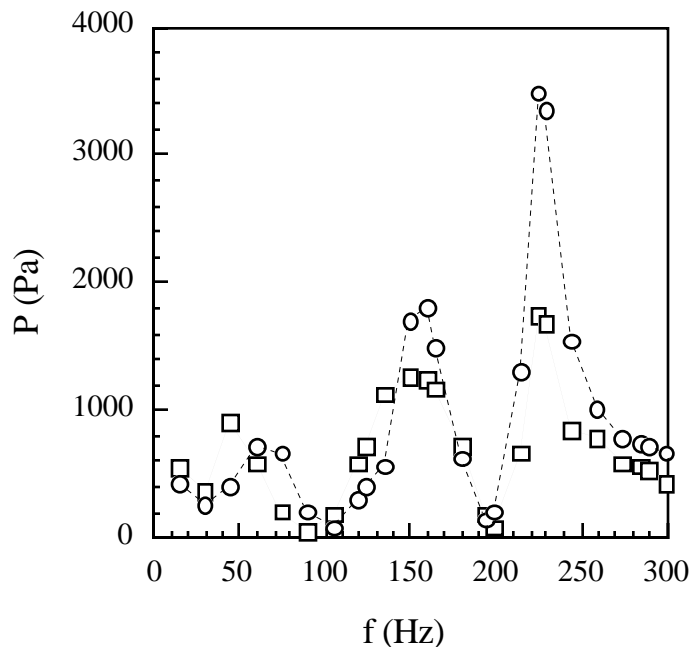


Figure 8: Effluent acoustic pressures for a constant acoustic source pressure amplitude of 812 Pa for the range of frequencies used in dissolution experiments. Circles with dotted lines represent experiments conducted with 1 mm beads and squares with solid lines represent experiments conducted with 2 mm bead column packings.

It should be noted that although a constant acoustic source pressure of 812 Pa was used, the effluent pressures were not constant for the different frequencies used. Moreover, it was found that the effluent pressures for both bead sizes followed the similar fluctuations as the observed ΔC 's (compare Figures 7 and 8). The effluent pressures were also observed to be greater for the case when the column was packed with 1 mm beads compared to being packed with 2 mm beads.

The relationship between ΔC and acoustic source pressures amplitudes, ranging from 0 to 1,625 Pa, for a constant frequency of 245 Hz was observed to increase with increasing pressure for both bead sizes (Figure 9). For the pressures analysed, ΔC ranged from 0 to 109 % for the 1 mm beads and 12 to 121 % for the 2 mm beads. Except for the greatest acoustic source pressure used (1,625 Pa), ΔC was again greater

for the case of 1 mm beads than the 2 mm beads. It should also be noted that an additional experiment was performed for the case of 2 mm beads at approximately 800 Pa and the results were almost identical, signifying experimental reproducibility.

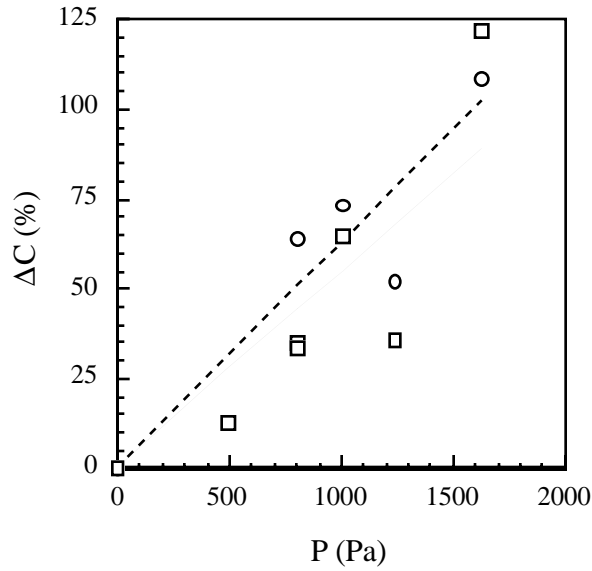


Figure 9: Effect of acoustic source pressure amplitude on percent change in effluent concentration for a constant acoustic frequency of 245 Hz. Circles with best fit dotted lines represent experiments conducted with 1 mm beads and squares with solid best fit lines represent experiments conducted with 2 mm bead column packings.

The experimental Br^- breakthrough data collected in this study indicate that acoustic waves enhance the transport of solutes in water saturated porous media. The degree of solute transport enhancement was found to be inversely proportional to the acoustic wave frequency. Due to experimental limitations, the characteristic acoustic wave frequency leading to a maximum enhancement of solute transport was not determined. However, it is assumed that this characteristic acoustic frequency, for the experimental conditions considered in this study, is within the range of the lowest frequency examined (60 Hz) and the base case (0 Hz).

Results from this research conclude that the use of acoustic pressure waves, complementing traditional pump-and-treat methodology, may be a viable method to decrease remediation times and costs for DNAPL contaminated aquifers. Increases in effluent concentration were observed to be over 100% greater by the addition of acoustic pressure waves which cause an effective pore water velocity for specific frequencies and pressures. The increase in effluent concentration was also found to be proportional to the applied acoustic source pressure and inversely proportional to bead diameter. Greater concentration increases for the smaller bead size was attributed to greater DNAPL-water interfacial areas based on smaller available pore spaces. No evidence of mobilization was observed in any experiment.

The experimental results suggest that further research should be undertaken to discern the governing mechanisms responsible for the enhanced transport and dissolution phenomenon. The preliminary findings of this study however, may be regarded as the initial step to the development of a clean groundwater remediation method as an alternative to currently available remediation methods.

REFERENCES

- Beresnev, I. A. and P. A. Johnson, Elastic-wave stimulation of oil production: A review of methods and results, *Geophysics*, 59(6), 1000–1017, 1994.
- Biot, M. A., Theory of propagation of elastic waves in a fluid-filled porous solid. I. Low-frequency range, *J. Acoust. Soc. Am.*, 28(2), 168–178, 1956a.
- Biot, M. A., Theory of propagation of elastic waves in a fluid-filled porous solid. II. High-frequency range, *J. Acoust. Soc. Am.*, 28(2), 179–191, 1956b.
- Brandes, D. and K. J. Farley, Importance of phase behavior on the removal of residual DNAPLs from porous media by alcohol flooding, *Water Environ. Res.*, 65(7), 869–878, 1993.
- Chaudhry, G. R., *Biological Degradation and Bioremediation of Toxic Chemicals*, 515 pp., Dioscorides Press, Portland, 1994.
- Chrysikopoulos, C. V., Artificial tracers for geothermal reservoir studies, *Environ. Geol.*, 22, 60–70, 1993.
- Chrysikopoulos, C. V., Effective parameters for flow in saturated heterogeneous porous media, *J. Hydrol.*, 170, 181–198, 1995.
- Chrysikopoulos, C. V., Three-dimensional analytical models of contaminant transport from nonaqueous phase liquid pool dissolution in saturated subsurface formations, *Water Resour. Res.*, 31(4), 1137–1145, 1995.
- Chrysikopoulos, C. V., P.K. Kitanidis, and P. V. Roberts, Analysis of one-dimensional solute transport through porous media with spatially variable retardation factor, *Water Resour. Res.*, 26(3), 437–446, 1990.

- Chrysikopoulos, C. V., P.K. Kitanidis, and P. V. Roberts, Generalized Taylor–Aris moment analysis of the transport of sorbing solutes through porous media with spatially–periodic retardation factor, *Transp. Porous Media*, 7(2), 163–185, 1992.
- Chrysikopoulos, C. V., K. Y. Lee, and T. C. Harmon, Dissolution of a well–defined trichlorethylene pool in saturated porous media: Experimental design and aquifer characterization, *Water Resour. Res.*, 36(7), 1687–1696, 2000.
- Dela Barre, B. K., T. C. Harmon, and C. V. Chrysikopoulos, Measuring and modeling the dissolution of nonideally shaped dense nonaqueous phase liquid pools in saturated porous media, *Water Resour. Res.*, 38(8), 1–13, 2002.
- de Marsily, G., *Quantitative Hydrogeology, Groundwater Hydrology for Engineers*, 440 pp., Academic Press, San Diego, California, 1986.
- Domenico, P. A. and F. W. Schwartz, *Physical and Chemical Hydrogeology*, 824 pp., Wiley, New York, 1990.
- Fortin, J., W. A. Jury, and M. A. Anderson, Enhanced removal of trapped non-aqueous phase liquids from saturated soil using surfactant solutions, *J. Contam. Hydrol.*, 24, 247–267, 1997.
- Geerits, T. W. and O. Kelder, Acoustic wave propagation through porous media: Theory and experiments, *J. Acoust. Soc. Am.*, 102(5), 2495–2510, 1997.
- Imhoff, P. T., P. R. Jaffe, and G. G. Pinder, An experimental study of complete dissolution of nonaqueous phase liquid in saturated porous media, *Water Resour. Res.*, 30, 307–320, 1994.
- IMSL, *IMSL MATH/LIBRARY user’s manual*, 2.0, IMSL, Houston, 1991.

- Kabala, Z. J., and G. Sposito, A stochastic model of reactive solute transport with time-varying velocity in a heterogeneous aquifer, *Water Resour. Res.*, 27(3), 341–350, 1991.
- Kreft, A. and A. Zuber, On the physical meaning of the dispersion equation and its solutions for different initial and boundary conditions, *Chem. Eng. Sci.*, 33, 1471–1480, 1978.
- Li, A., A. W. Andren, and S. H. Yalkowsky, Choosing a cosolvent; Solubilization of naphthalene and cosolvent property, *Environ. Toxicol. Chem.*, 15(12), 2233–2239, 1996.
- Mason, A. R. and B. H. Kueper, Numerical simulation of surfactant-enhanced solubilization of pooled DNAPL, *Environ. Sci. Tech.*, 30(11), 3205–3215, 1996.
- Parra, J. O. and P. Xu, Dispersion and attenuation of acoustic guided waves in layered fluid-filled porous media, *J. Acoust. Soc. Am.*, 95(1), 91–98, 1994.
- Powers, S. E., L. M. Abriola, W. J. Weber, An experimental investigation of non-aqueous phase liquid dissolution in saturated subsurface systems: steady-state mass transfer rates, *Water Resour. Res.*, 28, 2691–2705, 1992.
- Press, W. H., S. A. Teukolsky, W. T. Vetterling, and B. P. Flannery, Numerical Recipes in Fortran 90: The Art of Parallel Scientific Computing, 2nd ed., New York, Cambridge University Press, 1996.
- Santos, J. E., J. Douglas, Jr., J. Corbero, and O. M. Lovera, A model for wave propagation in a porous medium saturated by a two-phase fluid, *J. Acoust. Soc. Am.*, 87(4), 1439–1448, 1990.
- Tatalovich, M. E., K. Y. Lee, and C. V. Chrysikopoulos, Modeling the transport of contaminants originating from the dissolution of DNAPL pools in aquifers in the

- presence of dissolved humic substances, *Transp. Porous Media*, 38, 93–115, 2000.
- Valocchi, A. J., Spatial moment analysis of the transport of kinetically adsorbing solutes through stratified aquifers, *Water Resour. Res.*, 25(2), 273–279, 1989.
- Vogler, E. T. and C. V. Chrysikopoulos, Dissolution on nonaqueous phase liquid pools in anisotropic aquifer, *Stochastic Research and Risk Assessment*, 15, 33-46, 2001.
- Vogler, E. T. and C. V. Chrysikopoulos, Experimental investigation of acoustically enhanced solute transport in porous media, *Geophysical Research Letters*, 29(16), 10.1029/2002GL015304, 2002.
- Zhou, D., L. A. Dillard, and M. J. Blunt, A physically based model of dissolution of nonaqueous phase liquids in the saturated zone, *Transp. Porous Media*, 39, 227–255, 2000.